British Journal of Pharmacology

DOI:10.1111/bph.12691
www.brjpharmacol.org

RESEARCH PAPER

The TRPC channel blocker SKF 96365 inhibits glioblastoma cell growth by enhancing reverse mode of the Na^+/Ca^{2+} exchanger and increasing intracellular Ca^{2+}

M Song[1], D Chen[1] and S P Yu[1,2]

[1]*Department of Anesthesiology, Emory University School of Medicine, Atlanta, GA, USA, and* [2]*Department of Hematology and Oncology, Emory University School of Medicine, Atlanta, GA, USA*

Correspondence
Shan Ping Yu, 101 Woodruff Circle, Woodruff Memorial Research Building, Suite 620, Atlanta, GA 30322, USA. E-mail: spyu@emory.edu

Keywords
SKF 96365; TRPC channel; glioblastoma; calcium; Na^+/Ca^{2+} exchanger; cell cycle; cell death

Received
24 October 2013
Revised
26 February 2014
Accepted
11 March 2014

BACKGROUND AND PURPOSE

SKF 96365 is well known for its suppressing effect on human glioblastoma growth by inhibiting pre-activated transient receptor potential canonical (TRPC) channels and Ca^{2+} influx. The effect of SKF 96363 on glioblastoma cells, however, may be multifaceted and this possibility has been largely ignored.

EXPERIMENTAL APPROACH

The effects of SKF 96365 on cell cycle and cell viability of cultured human glioblastoma cells were characterized. Western blot, Ca^{2+} imaging and patch clamp recordings were used to delineate cell death mechanisms. siRNA gene knockdown provided additional evidence.

KEY RESULTS

SKF 96365 repressed glioblastoma cell growth via increasing intracellular Ca^{2+} ($[Ca^{2+}]_i$) irrespective of whether TRPC channels were blocked or not. The effect of SKF 96365 primarily resulted from enhanced reverse operation of the Na^+/Ca^{2+} exchanger (NCX) with an EC_{50} of 9.79 μM. SKF 96365 arrested the glioblastoma cells in the S and G_2 phases and activated p38-MAPK and JNK, which were all prevented by the Ca^{2+} chelator BAPTA-AM or EGTA. The expression of NCX in glioblastoma cells was significantly higher than in normal human astrocytes. Knockdown of the NCX1 isoforms diminished the effect of SKF 96365 on glioblastoma cells.

CONCLUSIONS AND IMPLICATIONS

At the same concentration, SKF 96365 blocks TRPC channels and enhances the reverse mode of the NCX causing $[Ca^{2+}]_i$ accumulation and cytotoxicity. This finding suggests an alternative pharmacological mechanism of SKF 96365. It also indicates that modulation of the NCX is an effective method to disrupt Ca^{2+} homeostasis and suppress human glioblastoma cells.

Abbreviations

$[Ca^{2+}]_i$, intracellular free Ca^{2+}; BDNF, brain-derived neurotrophic factor; ER, endoplasmic reticulum; NCX, Na^+/Ca^{2+} exchanger; SKF 96365, 1-[2-(4-methoxyphenyl)-2-[3-(4-methoxyphenyl)propoxy]ethyl-1H-imidazole hydrochloride; SOCE, store-operated Ca^{2+} entry; TRPC, transient receptor potential canonical

Introduction

Glioblastoma multiforme (GBM) or 'glioblastoma' is the most common and most aggressive malignant primary tumour originated from glia cells in the CNS (Brat *et al.*, 2008). Despite current therapeutic advances in solid cancers, the treatment of malignant glioblastoma remains highly unsatisfactory. Glioblastoma patients have a mean survival rate of 3–4 months after diagnosis, if no treatment is applied (Rao, 2003; Krex *et al.*, 2007). Under combined treatment of radiotherapy and chemotherapy, the median survival time for patients with grade IV glioblastoma can only be prolonged to 14.6 months (Stupp *et al.*, 2005; Van Meir *et al.*, 2010). It is thus necessary and important to identify new mechanisms that can inhibit proliferation and viability of glioblastoma cells and discover new targets to develop efficient tumour-suppressing strategies (Furnari *et al.*, 2007).

Intracellular free Ca^{2+} ($[Ca^{2+}]_i$) acts as a second messenger to regulate various signalling pathways (Berridge *et al.*, 2000; Clapham, 2007). Among Ca^{2+}-activated pathways, the MAPKs modulate many transcription factors and cell cycle in mammalian cells (Rosen *et al.*, 1994; Ashwell, 2006). Intracellular Ca^{2+} homeostasis is maintained by Ca^{2+}-permeable ion channels, receptors, Ca^{2+} pumps and Na^+/Ca^{2+} exchangers (NCX; transporter nomenclature follows Alexander *et al.*, 2013a) located in the plasma membrane and membranes of intracellular organelles (Verkhratsky *et al.*, 1998; Blaustein *et al.*, 2002). Genomic analyses of human glioblastoma revealed a number of altered functional genes, including enriched Ca^{2+} transporters (Furnari *et al.*, 2007; Parsons *et al.*, 2008). The Ca^{2+}-permeable transient receptor potential canonical (TRPC) channels are overexpressed in human glioblastoma specimens compared with normal brain tissues (Chigurupati *et al.*, 2010; Ding *et al.*, 2010; channel nomenclature follows Alexander *et al.*, 2013b). Ca^{2+} entry was functionally augmented through up-regulated TRPC6, and the elevated $[Ca^{2+}]_i$ was a necessary component for malignant growth of glioblastomas. In many previous reports, 1-[2-(4-methoxyphenyl)-2-[3-(4-methoxyphenyl) propoxy]ethyl-1H-imidazole hydrochloride (SKF 96365) was used to suppress proliferation of glioblastoma cells, and its anti-tumour effect has been attributed to an inhibitory effect on Ca^{2+} entry via TRPC or TRPC6 channels (Bomben and Sontheimer, 2008; Chigurupati *et al.*, 2010; Ding *et al.*, 2010). According to the International Union of Basic and Clinical Pharmacology (IUPHAR) database, SKF 96365 (~25 μM) is a pore blocker or antagonist for TRPC6 and TRPC7 (Harmar *et al.*, 2009). Because some subtypes of TRP channels are molecular components of store-operated Ca^{2+} entry (SOCE) channels, SKF 96365 is also described as a blocker of SOCE channels (Smyth *et al.*, 2006; Abramowitz *et al.*, 2007; Cheng *et al.*, 2013). In most studies, TRPC channels are routinely activated first by its agonists to induce intracellular Ca^{2+} elevation, and SKF 96365 is co-applied with the agonist to show attenuated Ca^{2+} entry via these channels (Bomben and Sontheimer, 2008; Chigurupati *et al.*, 2010; Ding *et al.*, 2010). Meanwhile, the effect of SKF 96365 on cell growth is usually examined under the condition that cell proliferation is already augmented by pre-activation of TRPC channels (Bomben and Sontheimer, 2008; Chigurupati *et al.*, 2010; Ding *et al.*, 2010). Based on these observations, TRPC/SOCE channels are suggested as a primary target for suppressing glioblastoma growth. Ironically, the direct action of SKF 96365 in glioblastoma cells, without activation of TRPC channels, has rarely been specifically examined.

Differing from reported inhibitory effect of SKF 97365 on Ca^{2+} entry, a few earlier studies indicated that when applied at similar concentrations for TRPC blockade, SKF 96365 could increase $[Ca^{2+}]_i$ through inhibition of the endoplasmic reticulum (ER) Ca^{2+} pump in epithelial cells, MDCK cells and some cancer cells (Schwarz *et al.*, 1994; Iouzalen *et al.*, 1996; Jan *et al.*, 1999). Leung *et al.* reported that in human leukemic HL-60 cells, SKF 96365 promotes Ca^{2+} entry from extracellular space and caused sustained $[Ca^{2+}]_i$ elevation via unknown mechanisms (Leung *et al.*, 1996). Elevation of $[Ca^{2+}]_i$ can be cytotoxic to many cells, including human cancer cells like glioblastoma cells (Lee *et al.*, 1994; Berridge *et al.*, 1998; Roderick and Cook, 2008). Unfortunately, the mechanism of this $[Ca^{2+}]_i$ increase induced by SKF 96365 and its potential cytotoxicity in anti-tumour property has not been carefully evaluated and specifically examined.

The NCX is a bidirectional transporter that normally extrudes Ca^{2+} from the intracellular space (forward mode), but may also bring Ca^{2+} into the cell (Ca^{2+} uptake) by a reversed operation (Yu and Choi, 1997; Annunziato *et al.*, 2004; DiPolo and Beauge, 2006). In recent years, Ca^{2+} entry carried by the reverse operation of the NCX under stress conditions has drawn increasing attention (Verkhratsky *et al.*, 1998; Kuhn *et al.*, 2009). It is possible that alterations in the direction of the NCX activity could present feasible methods of disrupting Ca^{2+} homeostasis and affecting the fate of tumour cells.

The present investigation explored the effect of SKF 96365 on $[Ca^{2+}]_i$ changes over the same concentration range as used for TRPC blockade and delineated the underlying mechanism in suppressing glioblastoma cells. We provide novel evidence that SKF 96365 suppressed growth of glioblastoma cells via a direct action of enhancing the reverse operation of the NCX and increasing intracellular Ca^{2+}. We also found that the expression of NCX isoforms was noticeably higher in glioblastoma cells than in normal astrocytes. Knockdown of NCX1 in glioblastoma cells diminished the effect of SKF 96365. These data suggested that the NCX could be a novel target for suppressing glioblastoma cells. Our findings should also have a major impact on studies using SKF 96365 as a pharmacological tool or therapeutic reagent in cell biology and anti-cancer treatments.

Methods

Culture of human glioblastoma cells and astrocytes

The human glioblastoma cell lines LN-229, T98G and U373 were obtained from Dr. Erwin G. Van Meir (Emory University, Winship Cancer Institute, Atlanta, GA, USA) and was characterized as previously described (Van Meir *et al.*, 1990; 1992). Glioblastoma cells were cultured in DMEM containing L-glutamine and 10% FBS. Human astrocytes were purchased from ScienCell Research Laboratories (Carlsbad, CA, USA) and cultured in human astrocyte medium supplemented

with 10% FBS and astrocyte growth supplement. After selecting for astrocytes in passage 1, passages 2–5 of human astrocytes were used for experiments. One hundred units·mL^{-1} penicillin and 0.1 mg·mL^{-1} streptomycin were routinely added into cell culture medium. Cells were maintained at 37°C in an incubator with a humidified atmosphere containing 5% CO_2/95% air.

Cell viability assay

The viability of cultured cells was measured with the 3-(4,5-dimethylthiazol-2-yl)-2,5-diphenyltetrasodium bromide (MTT; Sigma-Aldrich Corporation, St. Louis, MO, USA) assay. Briefly, cells were harvested from flasks and plated in 96-well cell culture plates at ~5×10^3 per well. Cells were treated with test reagents for 24 or 48 h. Control cells were treated with cell culture medium and measured at the same time point as treatment groups. MTT was added to each well at a final concentration of 0.5 mg·mL^{-1}. Four hours later, MTT formazan crystals generated by viable cells were dissolved in solubilization solution (10% SDS in 0.01 M-HCl) for 12 h at room temperature and absorbance was visualized at 560 nm. Results are expressed as the percentage of MTT values of treated groups versus control conditions.

Ca^{2+} imaging

LN-229 cells were cultured in 96-well plates and loaded with the cell membrane permeable Ca^{2+} dye Fluo-4 AM (5 μM) in 100 μL HEPES-buffered solution for 50 min. The solution contained (in mM): 135 NaCl, 3 KCl, 2 $CaCl_2$, 1 $MgCl_2$, 10 glucose and 10 HEPES, supplemented with 1% FBS at pH 7.4. To prepare the Ca^{2+}-free solution, 2 mM $CaCl_2$ was replaced with 1 mM EGTA in the HEPES-buffered solution. To initiate the reverse mode (Ca^{2+} uptake) of the NCX, we applied a modified Na^+-free solution (in mM): 130 KCl, 10 $CaCl_2$, 1 $MgCl_2$, 10 glucose and 10 HEPES, supplemented with 0.02 uabain (Na^+/K^+ ATPase inhibitor), 0.001 thapsigargin (ER Ca^{2+} pump inhibitor) and 0.01 nifedipine (voltage-gated Ca^{2+} channel blocker) (Kim *et al.*, 2005; Rahman *et al.*, 2012). The 96-well plate containing the Fluo-4 AM-loaded cells was mounted in an inverted fluorescence microscope (Olympus IX81, Olympus America Inc., Center Valley, PA, USA). Visual inspection and fluorescent imaging were carried out at room temperature. Fluo-4 epifluorescence was excited at 480 nm and images were collected from 520 nm emitted light with a CCD camera following the manufacturer's instructions (Fluo-4 NW Calcium Assay Kit; Invitrogen). The imaging data were recorded with a digital camera HAMAMATSU ORCA-ER (Hamamatsu Photonics K.K., Hamamatsu City, Japan) and analysed with the software Slidebook 4.1 for Windows (SciTech Pty Ltd, Preston, Victoria, Australia).

Cell cycle assay

The LN-229 cells were plated on 60-mm dishes (Corning Inc., Corning, NY, USA) and were treated with SKF 96365 or other drugs. The control group was treated with cell culture medium. After treatment, cells were trypsinized, harvested in 15 mL tubes and washed with sterile PBS. After centrifuging, cells were fixed with 70% ethanol for 30 min at room temperature. For propidium iodide (PI) staining, cells were washed three times with PBS and then were treated with RNase (100 μg·mL^{-1}) for 1 h. PI (10 μg·mL^{-1}) was added and stained cells were kept in the dark at 4°C until analysis. FACS analysis was performed using a BD Biosciences LSR II flow cytometer and FlowJo version 7.6 software (Tree Star, Ashland, OR, USA).

Western blot analysis

A Western blot analysis of cell extract was conducted as previously described (Zhou *et al.*, 2011). The primary antibodies for phosphorylated and total ERK, JNK and p38-MAPK were used. Antibodies for NCX1, NCX2 and NCX3 were used. Mouse β-actin antibody (Sigma-Aldrich Corporation) and α-tubulin antibody (Santa Cruz Biotechnology, Dallas, TX, USA) was used as protein loading controls.

Protein knockdown by siRNA

Following the guidelines of Invitrogen Life Technologies for transfection, LN-229 cells were transfected with 50 nM NCX1 siRNA (human SLC8A1; Invitrogen, 5′-CCC UGU UAG UAA GAU CUU CUU UGA A-3′) or negative control siRNA (Invitrogen) with Lipofectamine 2000 (Invitrogen) in Opti-MEM® Reduced Serum Medium (Gibco Life Technologies, Grand Island, NY, USA). Cells were analysed 24 and 48 h after siRNA treatment, and the efficacy of protein knockdown was detected by Western blot analysis of NCX1 proteins.

Whole-cell patch clamp recording

Whole-cell patch clamp recording was performed using an EPC9 amplifier (HEKA Elektronik, Lambrecht, Germany) at room temperature (Zhou *et al.*, 2011). The external solution had a pH of 7.4 and contained (in mM): 135 NaCl, 1.25 NaH_2PO_4, 1 $MgCl_2$, 2 $CaCl_2$, 10 HEPES, 10 glucose, 0.001 tetrodotoxin, 0.02 ouabain and 0.01 nifedipine. Internal solution consisted of (in mM): 120 CsCl, 20 NaCl, 2 $MgCl_2$, 13 $CaCl_2$, 2 Na_2ATP, 20 BAPTA and 10 HEPES at a pH 7.2. Recording electrodes pulled from borosilicate glass pipettes (Sutter Instrument, Novato, CA, USA) had a tip resistance between 6 and 8 MΩ when filled with the internal solution. Series resistance was compensated by 75–85%. Linear leak and residual capacitance currents were subtracted online using a P/6 protocol of the Pulse acquisition software (HEKA Elektronik). For the recording of the membrane currents mediated NCX, cells were held at −50 mV and depolarized to +60 mV, and then a voltage ramp starting from +60 to −120 mV was applied for 1000 ms before returning back to −50 mV (He *et al.*, 2003; Molinaro *et al.*, 2008; Rahman *et al.*, 2012). The reverse and forward NCX currents were measured at +50 and −110 mV potentials respectively (Molinaro *et al.*, 2008; Rahman *et al.*, 2012). For drug application, cells were perfused with an 8-channel MilliManifold (ALA MLF-8, ALA Scientific Instruments, Inc. Farmingdale, NY, USA) connected to a gravity-fed perfusion systems. Data were filtered at 3 KHz and digitized at sampling rates of 20 KHz.

Data analysis

Data are expressed as means ± SEM. The equilibrium potential of NCX, $E_{Na,Ca}$, was calculated by the following equation: $E_{Na,Ca} = 3E_{Na} - 2E_{Ca}$, where E_{Na} and E_{Ca} were the equilibrium potential of Na^+ and Ca^{2+} given by the Nernst equation. The concentrations of the SKF 96365 exerting half-maximal

enhancement of NCX (EC_{50}) were obtained by fitting the concentration–response with the equation: I/I_0*100% = Bottom+ (Top – Bottom)/[1 + 10^((LogEC50-C)*n)], where I_0 and I are current amplitudes measured in control and in the presence of SKF 96365, C is the logarithm of concentration and n is the Hill coefficient (GraphPad Prism 4.01; La Jolla, CA, USA). The fractional enhancement (f) was determined with the equation: $f = (I/I_0 - 1)$*100%. Comparisons between two groups was performed using Student's t-test. Multiple comparisons among groups were done by one-way ANOVA followed by a *post hoc* Tukey's test. Differences were considered to be significant at $P < 0.05$, and very significant at $P < 0.01$.

Materials

1-[2-(4-Methoxyphenyl)-2-[3-(4-methoxyphenyl)propoxy] ethyl-1H-imidazole hydrochloride (SKF 96365), BAPTA-AM, YM-244769, human brain-derived neurotrophic factor (BDNF) and thapsigargin were purchased from Tocris Bioscience (Minneapolis, MN, USA). PD169316 and SP600125 were obtained from (Sigma-Aldrich) SKF 96365 was dissolved in distilled deionized water to make a stock solution. EGTA and $NiCl_2$ were purchased from Sigma-Aldrich Corporation. Cell-permeable Fluo-4 AM was purchased from Invitrogen Life Technologies (New York, NY, USA). The primary antibodies for phosphorylated and total ERK, JNK and p38-MAPK were all purchased from Cell Signaling Technology (Boston, MA, USA). Anti-NCX1 antibody was purchased from Abcam, Inc. (Cambridge, MA, USA); anti-NCX2 and NCX3 antibodies were purchased from Alomone Labs (Jerusalem, Israel).

Results

SKF 96365-induced cell cycle arrest in human glioblastoma LN-229 cells

Human glioblastoma LN-229 cell cultures were treated with SKF 96365 at 0, 5, 10, 20 and 40 μM in DMEM containing 10% FBS. Cell cycle analysis of LN-229 cells stained with PI showed that incubation with SKF 96365 for 8 h significantly reduced the cell fraction in G_1 phase, and increased the proportion of cells in S phase of cell cycle in a concentration-dependent manner (Figure 1A and C). After 18 h treatment with SKF 96365, the cell fractions in both S and G_2 phases were significantly increased (Figure 1B,D). The MTT assay showed that 24 h treatment with SKF 96365 caused a concentration-dependent suppression of cell viability in LN-229 cell cultures (Figure 1E). Increasing the exposure to SKF 96365 to 48 h induced more cell death (Figure 1F).

The role of MAPK activation in SKF 9636-induced cell cycle arrest

MAPK family members play an important role in cell cycle regulation. We assessed the activities of ERK, p38-MAPK and JNK in glioblastoma cells at different time points after incubation with 20 μM SKF 96365 (Figure 2A). Western blot analysis of cell protein extracts showed that ERK was transiently activated after 10 min incubation with SKF 96365, and then returned to the baseline level at later time points. The activation of p38-MAPK was markedly increased 10 min after SKF 96365 incubation, peaked at 30 min and declined at 60 and 120 min after incubation, but still was significantly higher than the baseline level (Figure 2B). The activation of JNK also increased after 10 and 30 min incubation with SKF 96365, peaked at 60 min and declined to a level still higher than baseline at 120 min. In the control group, vehicle control (distilled deionized water) treatment did not affect the activities of ERK, p38-MAPK and JNK in glioblastoma cells over the same duration of SKF 96365 treatments (Figure 2C).

Because SKF 96365 markedly and more sustainably increased the activity of p38-MAPK and JNK but not ERK, we investigated whether or not p38-MAPK and JNK were involved in SKF 96365-induced cell cycle arrest of LN-229 cells. A p38-MAPK inhibitor, PD169316, and a JNK inhibitor, SP600125, were dissolved in DMSO to make stock solutions of 40 mM. In flow cytometry analysis, 18 h incubation with DMSO (1/1000, v/v), PD169316 (40 μM) or SP600125 (40 μM) did not induce significant cell fraction changes in G_1, S and G_2 phases of the cell cycle, while SKF 96365 (20 μM, 18 h) alone markedly decreased cell fraction in G_1 phase and increased cells in S and G_2 phases respectively (Figure 3A–D). Pretreatment of LN-229 cells with PD169316 (40 μM) or SP600125 (40 μM) prevented the action of SKF 96365 on the cell cycle profile, maintaining the cell fractions in G_1 S and G_2 phases at normal levels (Figure 3B,D). Thus, inhibition of p38-MAPK or JNK substantially prevented cell cycle arrest induced by SKF 96365, indicating their involvement in the effect of SKF 963656.

SKF 96365-induced $[Ca^{2+}]_i$ elevation in LN-229 cells

To characterize the effect of SKF 96365 on $[Ca^{2+}]_i$, LN-229 cells were preloaded with the Ca^{2+} indicator Fluo-4 AM (5 μM) and the change of $[Ca^{2+}]_i$ was normalized with control level. In the Ca^{2+}-containing solution supplemented with 1% FBS, application of SKF 96365 at 10, 20 and 40 μM induced concentration-dependent elevation of $[Ca^{2+}]_i$ (Figure 4A). To delineate the source of SKF 96365-induced $[Ca^{2+}]_i$ increase, SKF 96365 was tested in a Ca^{2+}-free solution (Ca^{2+} substituted by 1 mM EGTA). Under this condition, SKF 96365-induced $[Ca^{2+}]_i$ increase was greatly reduced at all three concentrations tested. In the absence of extracellular Ca^{2+}, SKF 96365 at 40 μM triggered a noticeable but much less pronounced $[Ca^{2+}]_i$ increase, which was transient and declined in a few minutes (Figure 4B). The area under the curve values showed that $[Ca^{2+}]_i$ elevation in the Ca^{2+}-free solution was less than half of that in Ca^{2+}-containing solutions (Figure 4C). These data indicate that SKF 96365-induced $[Ca^{2+}]_i$ elevation was mainly caused by Ca^{2+} influx from the extracellular space.

Several earlier reports suggest that SKF 96365 acts like thapsigargin to release Ca^{2+} from the ER Ca^{2+} stores by inhibiting the ER Ca^{2+} pump (Schwarz *et al.*, 1994; Iouzalen *et al.*, 1996; Leung *et al.*, 1996). To test this possibility, we first used 5 μM thapsigargin to trigger a robust $[Ca^{2+}]_i$ increase in LN-229 cells in the Ca^{2+}-free medium (Figure 4D). Subsequent application of 20 μM SKF 96365 did not induce any visible $[Ca^{2+}]_i$ increase (Figure 4D). A transient $[Ca^{2+}]_i$ increase was seen when SKF 96365 was applied before thapsigargin, and subsequent application of 5 μM thapsigargin still induced a significant Ca^{2+} increase (Figure 4E). This experiment agreed

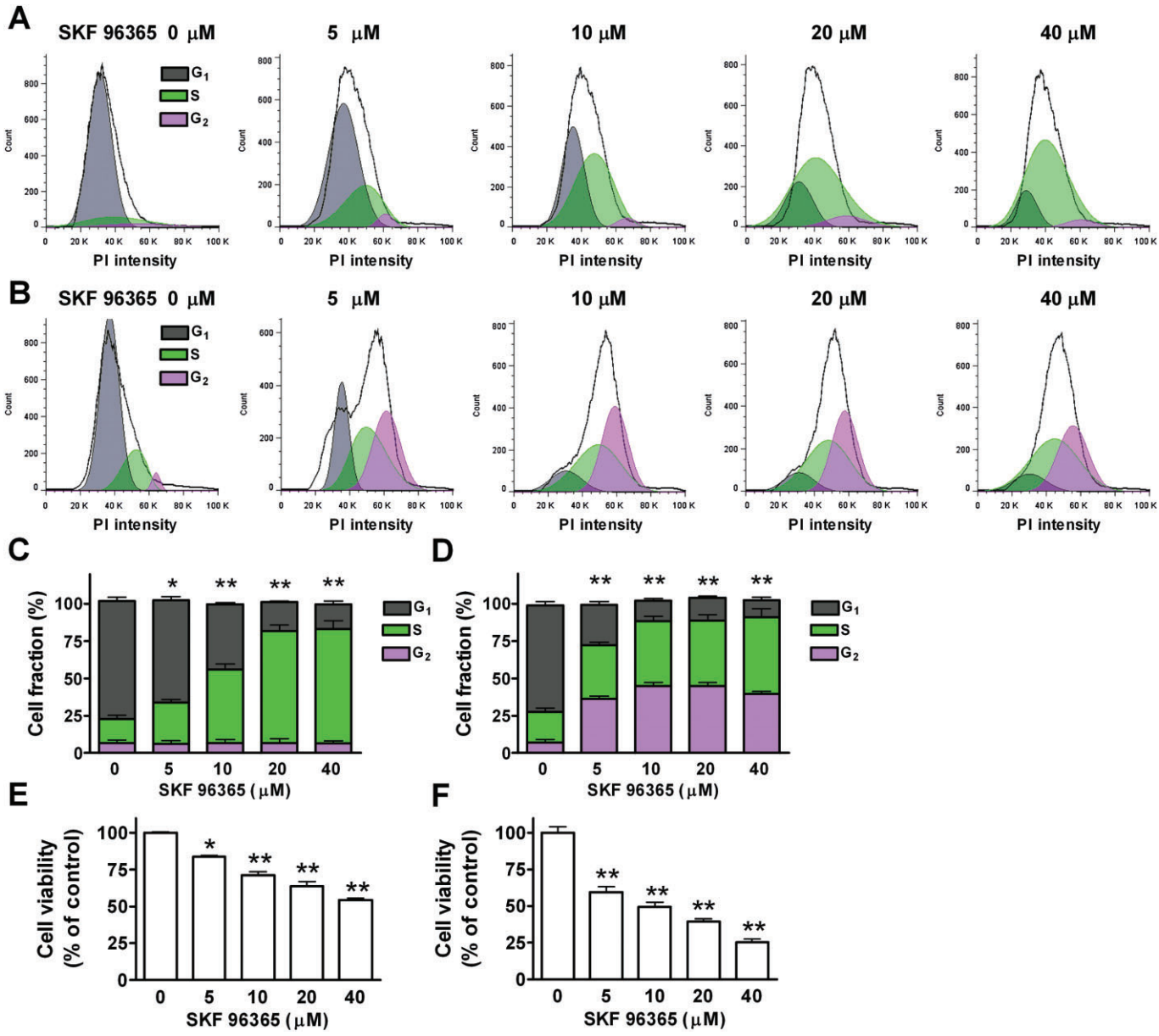

Figure 1

Effect of SKF 96365 on the cell cycle and viability of human glioblastoma cells LN-229. (A,B) Cell cycle assay of LN-229 cells after being incubated with SKF 96365 (0–40 μM) for 8 and 18 h. Cells were stained with PI and analysed with flow cytometry. (C,D) Cell fractions in G_1, S and G_2 phases of the cell cycle after being exposed to SKF 96365 (0–40 μM) for 8 and 18 h. $n = 5$ experiments in each group; $^*P < 0.05$; $^{**}P < 0.01$, cell fraction in G_1 phase of SKF 96365-treated groups compared with control group. (E) Viability of LN-229 cells after being exposed to SKF 96365 (0–40 μM) for 24 h. (F) Viability of LN-229 cells after 48 h treatment with SKF 96365. $n = 5$ in each group; $^*P < 0.05$; $^{**}P < 0.01$, compared with control group.

with the idea that SKF 96365 could act as a relatively weak ER Ca^{2+} pump inhibitor to release Ca^{2+} from the ER Ca^{2+} store.

SKF 96365 elevates $[Ca^{2+}]_i$ distinctive from its action on SOCE and TRPC6 channels

Previous studies using Ca^{2+} imaging of short durations (<10 min) showed that 3–30 μM SKF 96365 inhibited Ca^{2+} entry mediated by SOCE or TRPC in several cell lines (Merritt *et al.*, 1990; Wang and Poo, 2005; Jia *et al.*, 2007; Labelle *et al.*, 2007; Varnai *et al.*, 2009). We conducted Ca^{2+} imaging of 25–30 min on LN-229 cells in order to distinguish possible early and deferred effects of SKF 96365 on $[Ca^{2+}]_i$ homeostasis. Thapsigargin was used to trigger SOCE and BDNF was used to open TRPC channels in Ca^{2+}-containing solution (Lytton *et al.*, 1991; Li *et al.*, 2005; Amaral and Pozzo-Miller, 2007; Antigny *et al.*, 2011). In a solution containing 2 mM Ca^{2+}, 5 μM thapsigargin initially induced a rapid $[Ca^{2+}]_i$ increase followed by a slow decay, and finally this typical $[Ca^{2+}]_i$ elevation mediated by SOCE opening subsided to basal level after 20 min (Figure 5A). When SKF 96365 (20 μM) was co-applied

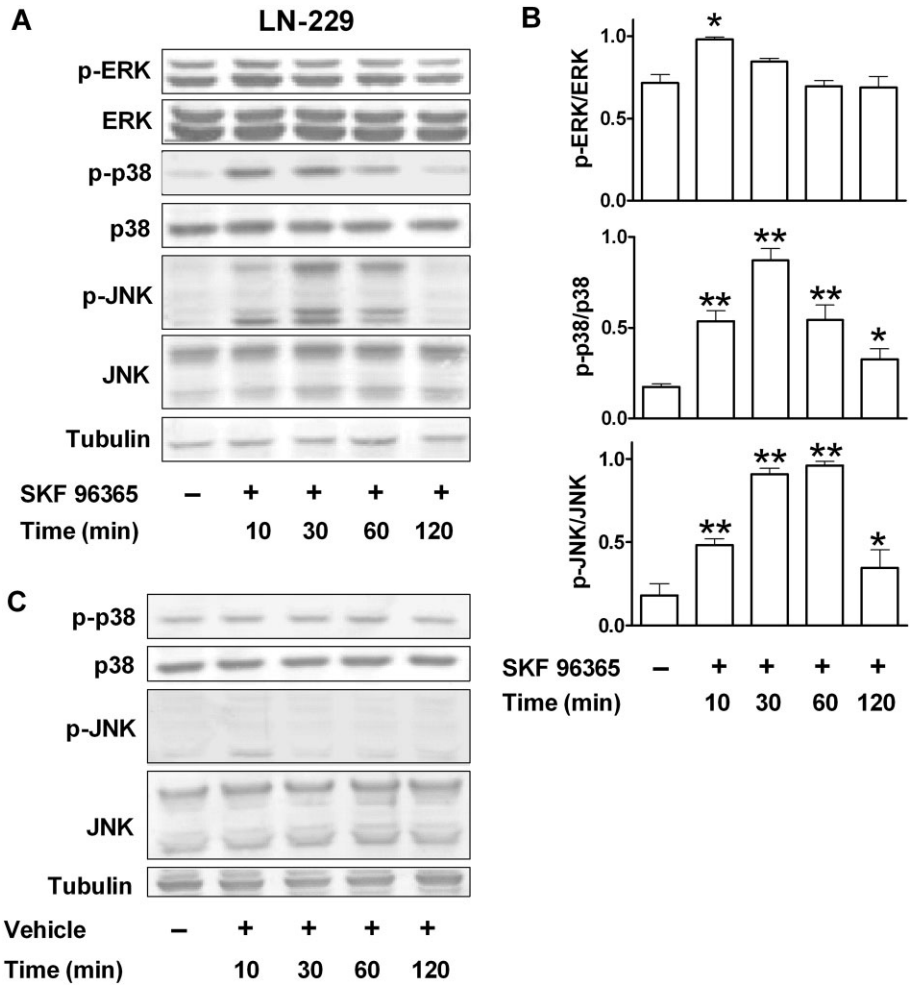

Figure 2

SKF 96365-induced activation of p38-MAPK and JNK. (A,B) LN-229 cells were treated with SKF 96365 at 20 μM for 10, 30, 60 and 120 min. The phosphorylated and total ERK, p38-MAPK and JNK were detected by Western blot. Tubulin was used as an internal control. $n = 4$ experiments in each group; *$P < 0.05$; **$P < 0.01$, SKF 96365-treated group compared with control group. (C) The activity of ERK, p38-MAPK and JNK after being treated with vehicle (distilled deionized water) for 10, 30, 60 and 120 min.

together with thapsigargin, the initial $[Ca^{2+}]_i$ increase disappeared but a slow $[Ca^{2+}]_i$ elevation succeeded (Figure 5A). BDNF-induced $[Ca^{2+}]_i$ elevation mediated by TRPC opening showed a slow decay during 30 min Ca^{2+} imaging. When SKF 96365 (20 μM) was applied 5 min after BNDF administration and TRPC activation, the BDNF-induced $[Ca^{2+}]_i$ elevation was suppressed and followed by a slow $[Ca^{2+}]_i$ elevation (Figure 5B). These Ca^{2+} imaging of longer duration revealed a novel evidence that although SKF 96365 initially inhibits SOCE or TRPC channels, it also triggers a belated and slow $[Ca^{2+}]_i$ elevation. Thus, SKF 96365 shows an effect of slowly enhancing intracellular Ca^{2+} in glioblastoma cells in a delayed fashion irrespective of whether SOCE and TRPC channels are blocked or not.

The role of $[Ca^{2+}]_i$ in SKF 96365-induced cell cycle arrest and MAPK activation

To determine the role of $[Ca^{2+}]_i$ increase in SKF 96365-induced cell cycle arrest, Ca^{2+} chelators EGTA and BAPTA-AM were used to arrest Ca^{2+} influx and prevent intracellular Ca^{2+} accumulation in LN-229 cells. Incubation with EGTA (2 mM) or BAPTA-AM (10 μM) alone for 18 h did not induce significant cell fraction changes in G_1, S and G_2 phases of the cell cycle (Figure 6A). The cell fraction in G_1 phase was markedly decreased by SKF 96365 (20 μM, 18 h) but in the presence of EGTA or BAPTA-AM, this treatment with SKF 96365 no longer affected the cell fraction in G_1 phase. Similarly, the cell fractions in S and G_2 phases remained close to control levels (Figure 6B).

We next examined the role of $[Ca^{2+}]_i$ in SKF 96365-induced MAPK activation. LN-229 cells were pretreated with Ca^{2+} chelator BAPTA-AM (10 μM) or EGTA (2 mM) for 18 h as well as during 30 min exposure to SKF 96365 (20 μM). Western blot analysis showed that the activation of p38-MAPK and JNK increased after 30 min incubation with SKF 96365 alone. Addition of BAPTA-AM or EGTA substantially suppressed SKF 96365-induced activation of p38-MAPK and JNK (Figure 6C,D). Thus, Ca^{2+} influx and $[Ca^{2+}]_i$

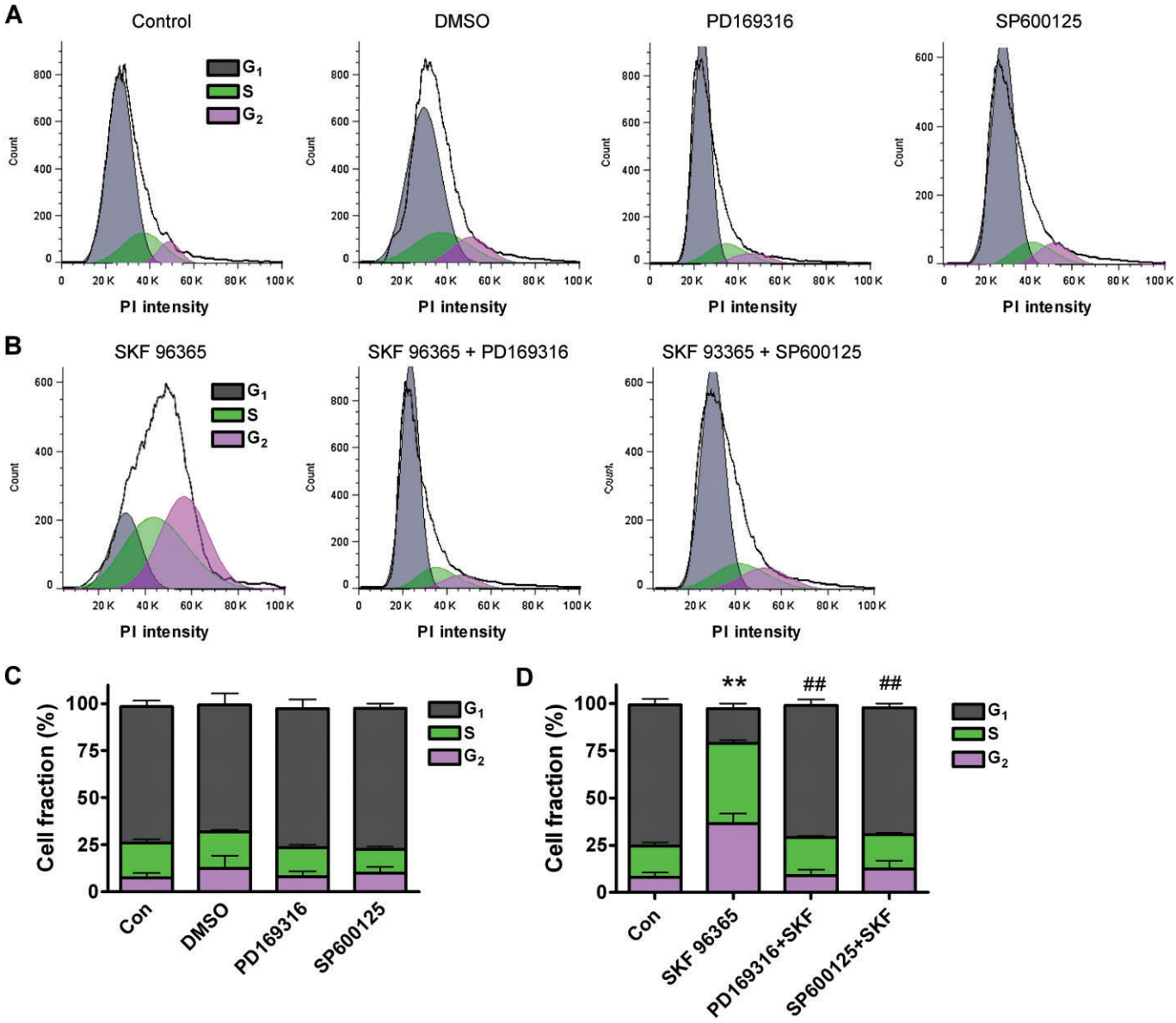

Figure 3

The role of p38-MAPK and JNK in SKF 96365-induced cell cycle arrest. (A) LN-229 cells were treated with DMSO (1/1000, v/v), PD169316 (40 μM) and SP600125 (40 μM) for 18 h. Cells were analysed with flow cytometry. (B) LN-229 cells were pretreated with PD169316 (40 μM) and SP600125 (40 μM) for 2 h, then incubated with SKF 96365 (20 μM) for 18 h and analysed with flow cytometry. (C,D) The cell fractions in G_1, S and G_2 phases of LN-229 cells after being exposed to treatments as indicated in each group. $n = 4$ experiments in each group; $^{**}P < 0.01$, cell fraction in G_1 phase of SKF 96365-treated group compared with control group. $^{\#\#}P < 0.01$, G_1 phase of SKF 96365-treated group compared with PD169316 or SP600125 pretreatment plus SKF 96365 groups.

elevation play a mediating role in SKF 96365-induced cell cycle arrest and MAPK activation. Cell viability assessed by MTT showed that 24 h treatment with EGTA (2 mM) or BAPTA-AM (10 μM) does not affect cell growth of LN-229 cells, while 24 h incubation with SKF 96365 (20 μM) greatly suppressed cell viability. Pretreatment with EGTA (2 mM) or BAPTA-AM (10 μM) for 2 h significantly diminished the suppressing effect of SKF 96365 on cell viability (Figure 6E).

SKF 96365 enhanced the NCX activity in its reverse mode

We next asked the question about which membrane molecule could mediate the Ca^{2+} influx upon SKF 96365 application. A previous study suggested that SKF 96365 might act on NCX and cause a direct Ca^{2+} entry in kidney cells (Jan *et al.*, 1999). There was, however, no characterization on how NCX was affected. Using whole-cell patch clamp recording, we measured the NCX activity associated membrane currents

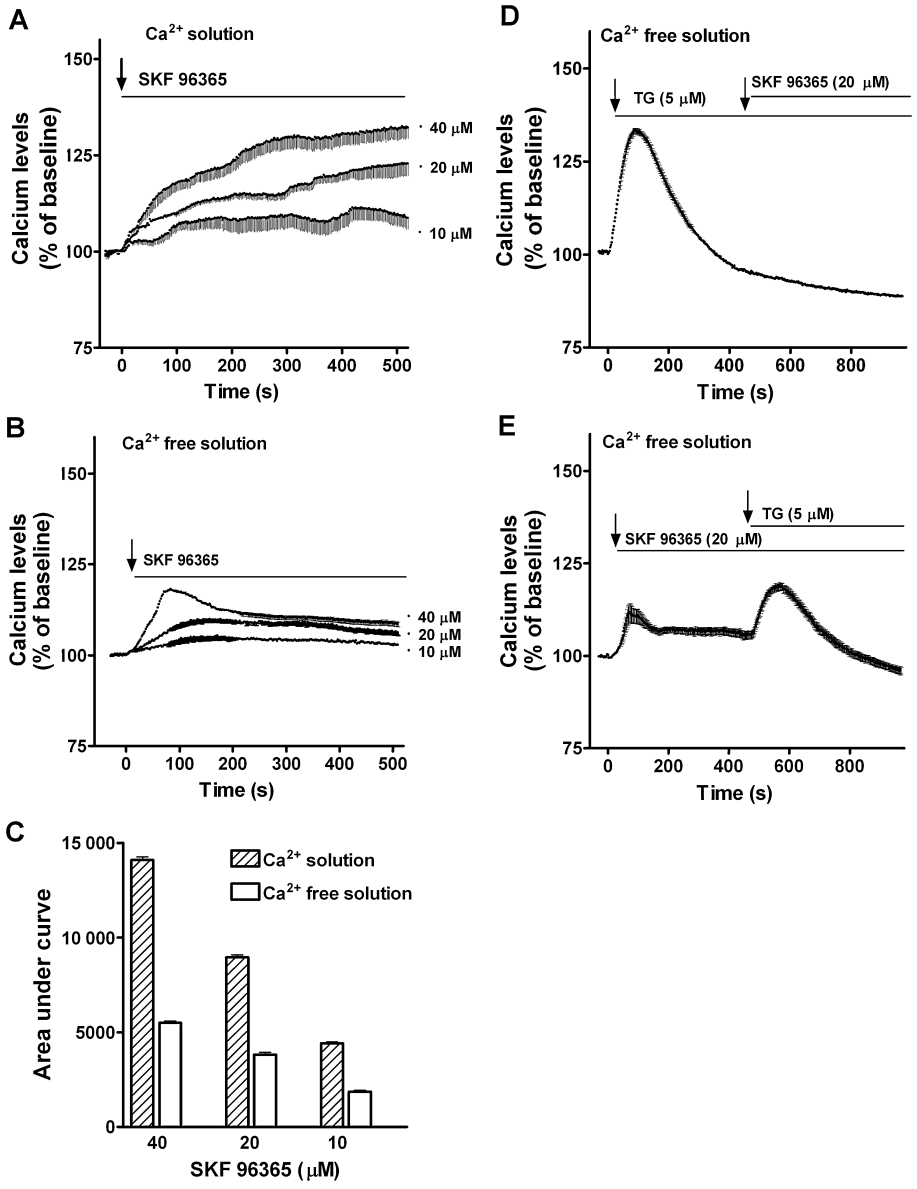

Figure 4

SKF 96365-induced intracellular Ca^{2+} elevation. (A) Fluo-4 AM-loaded cells were treated with SKF 96365 (10–40 μM) in the HEPES-buffered solution with 2 mM Ca^{2+}. (B) Ca^{2+} elevation caused by SKF 96365 (10–40 μM) in the HEPES-buffered solution without Ca^{2+}. (C) The area between 100% baseline and the curve of Ca^{2+} elevation induced by SKF 96365 (10–40 μM) in the solution with or without Ca^{2+}. (D) In the Ca^{2+}-free medium, cells were treated with thapsigargin (TG) for 500 s, then treated with SKF 96365 (20 μM) for another 500 s. (E) In the Ca^{2+}-free medium, cells were treated with SKF 96365 (20 μM) for 500 s, then treated with TG for another 500 s. $n = 4$ experiments in each test and 40–60 cells were imaged per experiment.

mediated by either forward or reverse modes. NCX currents were evoked by a voltage ramp from +60 to −120 mV in the presence of tetrodotoxin, ouabain and nifedipine. The amplitude of reverse and forward NCX currents was determined by the measurements at +50 and −110 mV respectively. The reverse and forward currents of NCX activation were substantially suppressed by the non-selective NCX blocker Ni^{2+} (10 mM) (Figure 7A). The reverse operation of NCX currents were inhibited by a selective inhibitor YM-244769 (Iwamoto and Kita, 2006) (Figure 7B). Interestingly, SKF 96365 enhances the NCX reverse mode currents in glioblastoma cells, while the forward mode current was much less affected (Figure 7C). The fractional enhancement (*f*) of the reverse NCX currents was 52.9 ± 22.9%, 84.9 ± 15.7% and 99.2 ± 13.7% when SKF 96365 was applied at 10, 100 and 300 μM respectively. Meanwhile, the *f* values of the NCX forward current were only 16.5 ± 9.5%, 22.3 ± 15.8% and 29.4 ± 14.8% at each higher concentration of SKF 96365. This SKF 96365-enhanced NCX current was suppressed by 10 mM Ni^{2+} (Figure 7D). The dose–response curve fitting yielded an EC_{50} of 9.79 μM for SKF 96365 to enhance the reverse-mode NCX currents (Figure 7E). The reversal potential (−61 mV) for NCX

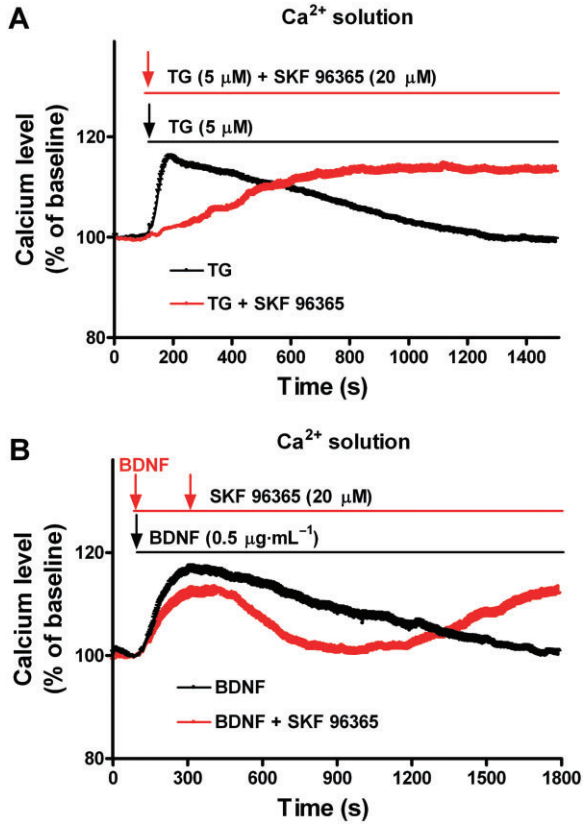

Figure 5

SKF 96365 elevates intracellular Ca^{2+} although it blocks SOCE and TRPC6 channels. (A) In the solution containing 2 mM Ca^{2+}, thapsigargin (TG) triggered a SOCE with a slow decay in LN-229 cells (black line, 25 min). Red line shows TG-induced Ca^{2+} entry is suppressed by SKF 96365, but after that a slow Ca^{2+} elevation occurs. (B) In the Ca^{2+} solution, BDNF triggered a Ca^{2+} entry (TRPC channel opening) with a slow decay (black line, 30 min). Red line shows BDNF-induced Ca^{2+} entry is suppressed by SKF 96365, but after that a slow Ca^{2+} elevation occurs. n = 4 experiments in each test and 30–53 cells were imaged per experiment.

was indicated by the intersection of current–voltage relation (I/V) in the absence and presence of Ni^{2+} (Figure 7F), which was close to the equilibrium potential (–69 mV) of NCX currents calculated based on the Nernst equation.

The function of reverse operation of the NCX is to take up Ca^{2+} from the extracellular space, resulting in increased $[Ca^{2+}]_i$ (Sokolow *et al.*, 2011; Verkhratsky *et al.*, 2012). Ca^{2+} imaging in LN-229 cells was used to test this effect. After 30 s of baseline recording in normal solution, the reverse mode of the NCX was evoked by application of a Na^+-free solution under the condition that Na^+/K^+-ATPase, ER Ca^{2+} pump and voltage-gated Ca^{2+} channels were already blocked (Kim *et al.*, 2005; Rahman *et al.*, 2012). Upon switching to the Na^+-free solution, a marked and transient $[Ca^{2+}]_i$ elevation occurred; however, this $[Ca^{2+}]_i$ increase was followed with a fast decay. When SKF 96365 (20 μM) was included in the Na^+-free solution, the $[Ca^{2+}]_i$ decay was abolished and a persistent $[Ca^{2+}]_i$ increase was observed (Figure 7G). In the normal Ca^{2+} solution, SKF 96365-induced $[Ca^{2+}]_i$ elevation was suppressed by YM-244769 (Figure 7H), which is a selective inhibitor for the reverse mode of NCX (Iwamoto and Kita, 2006). These data support that SKF 96365 enhances or sustains the reverse mode of the NCX in LN-229 cells.

Expression of NCX1, NCX2 and NCX3 in human astrocytes and glioblastoma cells

As there is no direct evidence regarding protein expression of NCX in human glioblastoma cells, we characterized the NCX expression in LN-229, T98G and U373 cell lines and compared them with normal human astrocytes. There are three major isoforms of NCX (NCX1, 2 and 3) expressed in neurons and astrocytes (Minelli *et al.*, 2007; Sokolow *et al.*, 2011). In Western blotting, the NCX1 antibody revealed three bands at 70, 120 and 160 kDa (Figure 8A), which was predicted in the manufacturer's data sheet and consistent with previous observations (Minelli *et al.*, 2007). The NCX2 antibody detected two bands at 100 and 60 kDa (Figure 8B), and the NCX3 antibody detected a band at 120 kDa (Figure 8C), which are all identical to existing reports (Thurneysen *et al.*, 2002; Minelli *et al.*, 2007; Sokolow *et al.*, 2011). Quantification of the band gray density showed that the expression of NCX1 and NCX2 were higher in three glioblastoma cell lines than that in normal astrocytes. A higher expression of NCX3 was also detected in LN-229 and T98G cells (Figure 8A–C).

Knockdown of NCX1 diminishes the effect of SKF 96365 on glioblastoma cells

The above data showed that SKF 96365 enhanced the reverse mode of NCX that is highly expressed in human glioblastoma cells. We speculated that down-regulation of NCX isoforms would affect or diminish the suppressing effect of SKF 96365 on glioblastoma cells. The specific siRNA (siNCX1) was used to knock down NCX1 expression in LN-229 cells. Negative control siRNA (siCTL) was used for comparison. Western blot analysis identified a significant decrease in the NCX1 protein level after 48 h siRNA transfection (Figure 9A). Consistently, patch clamp recording verified that the current density of the reversed activity of NCX was markedly decreased by 48 h siNCX1 incubation (Figure 9B). As expected, NCX1 knockdown significantly attenuated the SKF 96365 effect. The potentiating effect of SKF 96365 on the NCX reverse current was significantly attenuated in NCX1 knockdown cells (Figure 9C).

To further verify our hypothesis on the NCX role in cell cycle, we challenged siRNA-treated cells with SKF 96365 (20 μM) for another 24 h. Cell cycle assay showed that SKF 96365-induced cell cycle arrest in LN-229 cells was partially restored by NCX1 knockdown (Figure 9D). The cell fraction in G1 phase of knockdown control (siCTL) + SKF 96365 group was 21.9 ± 5.3; this value increased to 43.4 ± 5.8 in siNCX + SKF 96365 group. Cell viability assay showed that siCTL- and siNCX1-treated cells were all suppressed by SKF 96365 (Figure 9E). However, the viability of siNCX1-treated cells was significantly better than siCTL-treated cells, indicating that knockdown of NCX1 diminished the suppressing effect of SKF 96365 on glioblastoma cell growth.

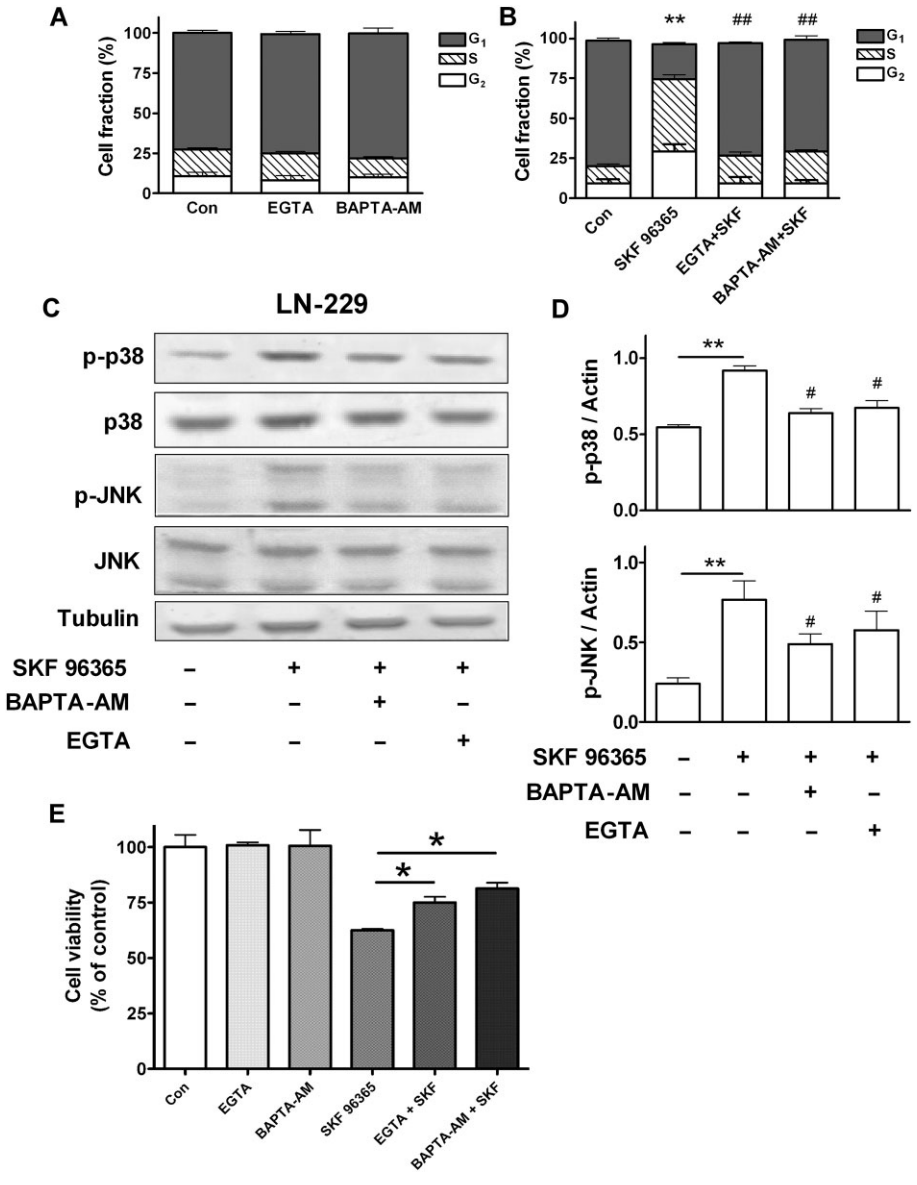

Figure 6

The mediating role of Ca^{2+} in SKF 96365-induced cell cycle arrest and MAPK activation. (A) LN-229 cells were treated with EGTA (2 mM) or BAPTA-AM (10 μM) for18 h and analysed with flow cytometry. (B) LN-229 cells were pretreated with EGTA (2 mM) or BAPTA-AM (10 μM) for 2 h, then incubated with SKF 96365 (20 μM) for 18 h. Cell fractions in G_1, S and G_2 phases were obtained from cell cycle analysis. $n = 4$ experiments in each group; $^{**}P < 0.01$, cell fraction in G_1 phase of SKF 96365-treated group compared with control group. $^{\#\#}P < 0.01$, cell fraction in G_1 phase of SKF 96365-treated group compared with PD169316 and SP600125 pretreatment plus SKF 96365 groups. (C,D) LN-229 cells were pretreated with BAPTA-AM (10 μM) or EGTA (2 mM) for 18 h, then incubated with SKF 96365 (20 μM) for 30 min. The phosphorylated and total p38-MAPK and JNK were analysed by Western blot. $n = 4$ experiments in each group; $^{**}P < 0.01$, SKF 96365-treated group compared with control group; $^{\#}P < 0.05$, SKF 96365-treated group compared with BAPTA-AM or EGTA pretreatment plus SKF 96365 groups. (E) Viability of LN-229 cells after 24 h treatment with EGTA (2 mM), BAPTA-AM (10 μM), SKF 96365 (20 μM), EGTA + SKF 96365 and BAPTA-AM + SKF 96365. $n = 5$ in each group; $^{*}P < 0.05$, SKF 96365-treated group compared with EGTA + SKF 96365 or BAPTA-AM + SKF 96365 group.

Discussion and conclusions

The TRPC or SOCE channel blocking action has been widely applied to elaborate SKF 96365-induced cell death mechanism in several cell lines. The present investigation provides novel evidence demonstrating a new mechanism for the tumour-suppressing effect of SKF 96365 on human glioblastoma cells. SKF 96365 induced cell cycle arrest of these tumour cells by arresting cells in the S and G_2 phases. This cell cycle arrest resulted from activation of p38-MAPK and JNK signalling. We further demonstrated that extracellular Ca^{2+} entry and intracellular Ca^{2+} elevation played a mediating role in SKF 96365-induced cell cycle arrest and MAPK activation. More interestingly, Ca^{2+} imaging analysis and electrophysi-

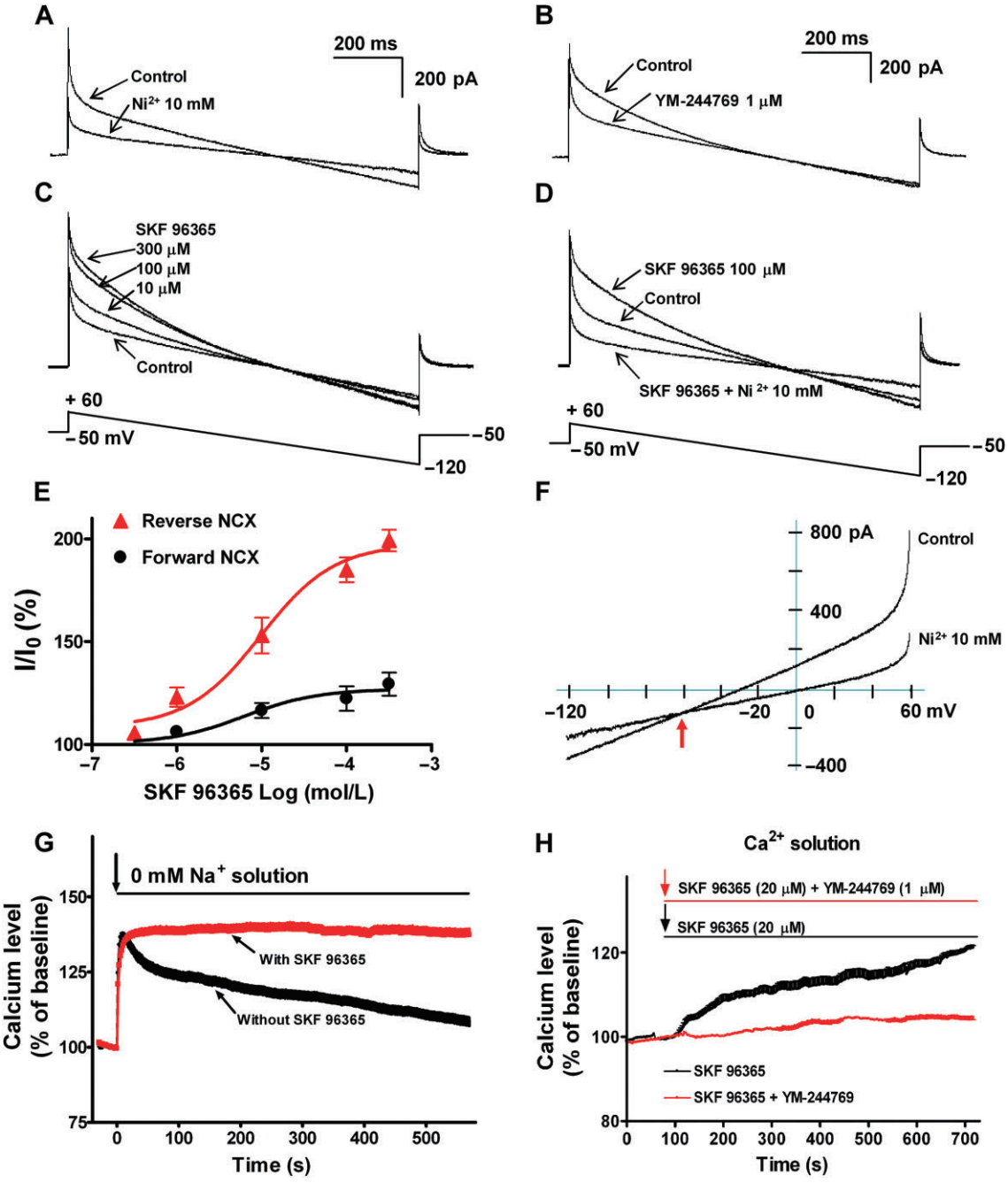

Figure 7

SKF 96365 enhances the reverse mode of NCX in glioblastoma cells. (A,B) LN-229 cells were held at −50 mV, the NCX currents were elicited by a ramp from +60 to −120 mV. Ni^{2+} (10 mM) and YM-244769 (1 μM) were used to inhibit NCX currents. (C) NCX currents recorded before and after application of SKF 96365 at 10, 100 and 300 μM. (D) NCX currents were enhanced by SKF 96365 and inhibited by Ni^{2+}. (E) Concentration–response curves of SKF 96365 acting on the NCX reverse (red) and forward mode currents. n = 6 for each dose point. (F) Intersection of current–voltage relation (I/V) of NCX in the absence and presence of Ni^{2+} yields a reversal potential of around −61 mV (indicated by red arrow). (G) The Na^+-free solution induced $[Ca^{2+}]_i$ elevation (Ca^{2+} uptake by the reverse mode of NCX) in the absence and presence of SKF 96365 (20 μM). (H) In the solution containing 2 mM Ca^{2+}, SKF 96365 induced intracellular Ca^{2+} changes in the absence and presence of YM-244769 (red). n = 4 experiments for Ca^{2+} imaging and 35–50 cells were imaged per test.

ological recordings showed that SKF 96365 enhanced the reverse mode of the NCX and thus led to $[Ca^{2+}]_i$ elevation irrespective of whether SOCE and TRPC channels are blocked or not. SKF 96365 showed this NCX regulatory action at the similar concentration that blocks TRPC or SOCE channels. In our patch clamp recording and Ca^{2+} imaging experiments, there was no TRPC agonist in the experimental solutions. Therefore, it is reasonable to assume that the data obtained

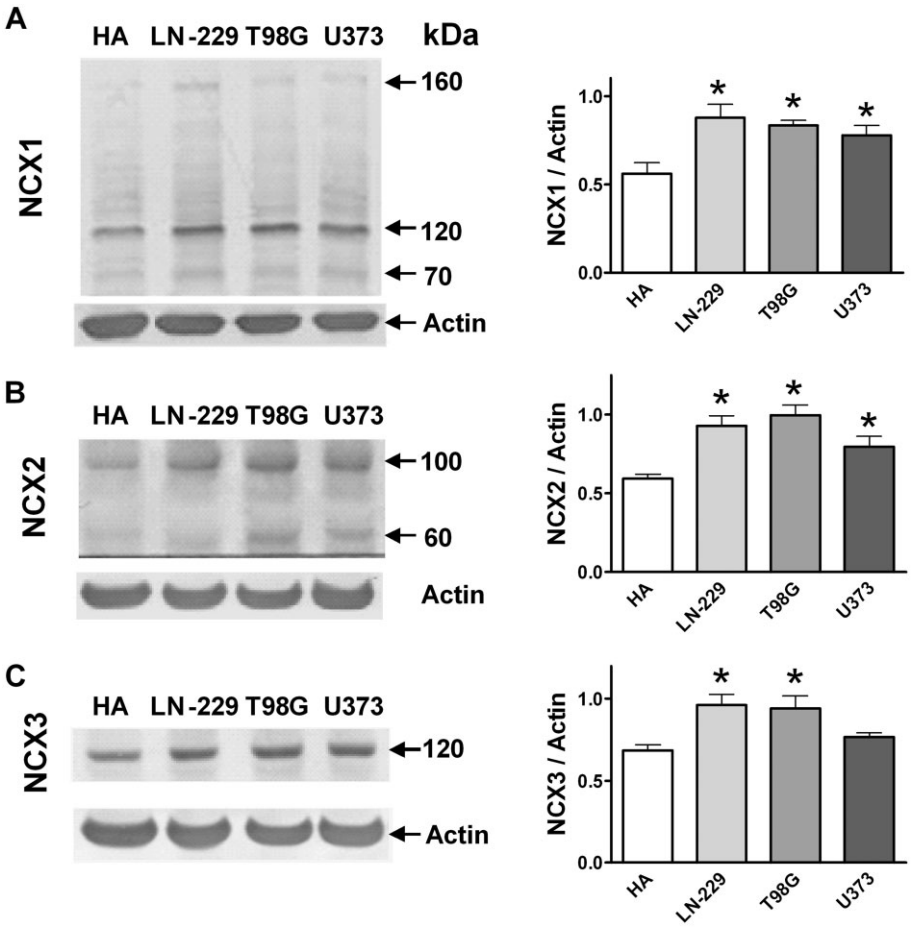

Figure 8

Expression of NCX isoforms in human astrocytes and glioblastoma cells. (A) From the samples of human astrocytes (HA), LN-229, T98G and U373 cells, anti-NCX1 antibodies revealed three bands at 70, 120 and 160 kDa (left panel). Right panel shows band gray density of glioblastoma cells and comparison to HA. *$P < 0.05$, compared with HA. (B) anti-NCX2 antibodies reveal two bands at 60 and 100 kDa (left panel). Right panel shows band gray density of each cell line. *$P < 0.05$, compared with HA. (C) anti-NCX3 antibodies reveal one band at 120 kDa (left panel). Right panel shows band gray density of each cell line. *$P < 0.05$, compared with HA. $n = 4$ experiments in each group.

from these experiments did not include effects due to TRPC activity. We also found that the expression of NCX subunits was noticeably higher in glioblastoma cells than that in normal human astrocytes and knockdown of the NCX1 isoforms in glioblastoma cells diminished the effect of SKF 96365. Thus, NCX subunits and regulation of its operation could be therapeutic targets for suppressing glioblastoma cell growth.

A general search in PubMed using the key word 'SKF 96365' produces over 600 research articles and the majority of them described SKF 96365 as a TRPC or SOCE channel blocker. These investigations in general have focused on the inhibitory effect of SKF 96365 on the Ca^{2+} entry via TRPC channels or SOCE (Merritt *et al.*, 1990; Labelle *et al.*, 2007; Bomben and Sontheimer, 2008; Chigurupati *et al.*, 2010; Ding *et al.*, 2010; Liu *et al.*, 2011). The action of SKF 96365 on the NCX and its associated regulation on Ca^{2+} homeostasis has never been directly tested before this investigation.

SKF 96365 inhibits proliferation of certain cancer cells including glioblastoma cells, human gastric and breast cancer cells (Bomben and Sontheimer, 2008; Cai *et al.*, 2009; Yang *et al.*, 2009; Liu *et al.*, 2011). We demonstrate here that SKF 96365 suppresses proliferation of human glioblastoma cells through elevating $[Ca^{2+}]_i$ rather than decreasing $[Ca^{2+}]_i$. More specifically, electrophysiological recording of the NCX-associated membrane currents and Ca^{2+} imaging show that the SKF 96363-induced $[Ca^{2+}]_i$ increase is achieved via an enhancement of the reverse mode of the NCX that are highly expressed in glioblastoma cells. It should be noted that when TRPC or SOCE channels are blocked by SKF 96365, Ca^{2+} ions can still enter into a cell through other routes such as the voltage-gated Ca^{2+} channels and Ca^{2+}-permeable receptors. In fact, it was seen in previous investigations that blocking TRPC channels by SKF 96365 cannot completely switch off Ca^{2+} influx into cytoplasm or prevent $[Ca^{2+}]_i$ increases (Li *et al.*, 2005; Jia *et al.*, 2007; Labelle *et al.*, 2007). This is consistent with the notion that there must be additional mechanism/s that mediated Ca^{2+} influx and $[Ca^{2+}]_i$ increase in the presence of SKF 96365. In our study, SKF 96365-induced cell cycle arrest resulted from $[Ca^{2+}]_i$ elevation and activation

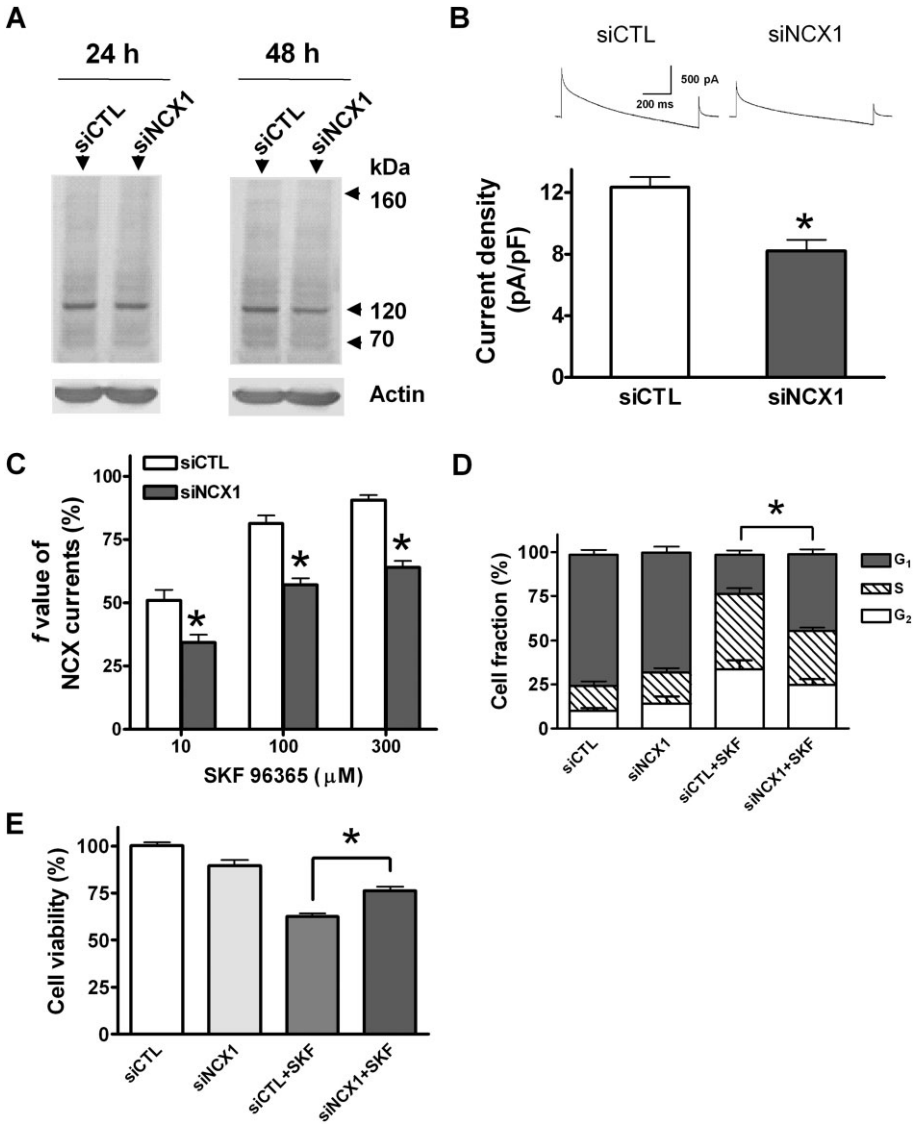

Figure 9

Knockdown of NCX1 diminishes the effect of SKF 96365 on glioblastoma cells. (A) Protein expression of NCX1 in LN-229 cells after 24 and 48 h treatment with negative control siRNA (siCTL) or NCX1 siRNA (siNCX1). (B) Current density of the reverse mode NCX in LN-229 cells after 48 h treatment with siCTL or siNCX1. $n = 6$. $^*P < 0.05$; comparison between the two groups. (C) After 48 h treatment with siCTL or siNCX1, the fractional enhancement (f) of the reverse mode NCX currents when SKF 96365 was applied at 10, 100 and 300 μM. $n = 6$. $^*P < 0.05$. (D) Cell cycle assay after 48 h treatment with siRNA and then being exposed to SKF 96365 (20 μM) for 24 h. $n = 4$ experiments in each group; $^*P < 0.05$; cell fraction in G_1 phase of LN-229 cells treated with siCTL + SKF 96365 compared with siNCX1 + SKF 96365 treatment. (E) Cell viability of LN-229 cells after 48 h treatment with siRNA and then being exposed to SKF 96365 (20 μM) for 24 h. $^*P < 0.05$; siCTL + SKF 96365 treatment compared with siNCX1 + SKF 96365 treatment. $n = 5$ experiments in each group.

of the p38-MAPK and JNK signalling. This type of $[Ca^{2+}]_i$ increase is not restricted to any particular micro-domain in a cell as we found that SKF 96365 induced a sustained $[Ca^{2+}]_i$ increase at room temperature. The amplitude of SKF 96365-induced $[Ca^{2+}]_i$ increase could be even higher in cells recorded at 37°C or under *in vivo* condition. Some reports showed that the amplitude of $[Ca^{2+}]_i$ rise correlates to MAPK activation (Ashwell, 2006). Moreover, MAPK may regulate cell cycle through NF-κB or phosphorylation of cyclin-dependent kinases (CDKs) (See *et al.*, 2004; Gutierrez *et al.*, 2010). The role of these signalling pathways in the effect of SKF 96365 remains to be examined.

It is important to point out that NCX is normally the major membrane protein responsible for Ca^{2+} extrusion (forward mode), regardless of the routes of $[Ca^{2+}]_i$ entry. The possibility that SKF 96365 might act on NCX was proposed by an early study performed on MDCK cells (Jan *et al.*, 1999). Unfortunately, this early report provided no direct evidence and did not characterize the action of SKF 96365 on the NCX (Jan *et al.*, 1999). Our study now provides direct and specific

evidence that SKF 96365 promotes the reverse operation of the NCX, which acts as a major underlying mechanism for disrupted Ca^{2+} homeostasis and cell death. The potentiation of reverse mode of NCX might result from depolarization of cell membrane. It is well known that the direction of operation of the NCX is voltage-dependent and it was reported that SKF-96365 could depolarize the membrane of smooth muscle (Annunziato *et al.*, 2004; Hotta *et al.*, 2005). Similar to genomic analyses reporting that Ca^{2+} transporter are up-regulated in human glioblastoma samples (Furnari *et al.*, 2007; Parsons *et al.*, 2008), the three NCX isoforms (NCX1, 2 and 3) are abundantly expressed in glioblastoma cells compared with normal human astrocytes. Our NCX knockdown experiments provided additional evidence to support our conclusion that SKF 96365 acts as an enhancer of the reverse mode of the NCX.

The findings of our investigation generate an unavoidable concern regarding the utilization of SKF 963635 as a pharmacological tool to block TRPC or SOCE channels and induce cell death. It should be taken into account that SKF 96365-caused cell death, especially in cancer cells where NCX is highly expressed, may result from $[Ca^{2+}]_i$ elevation but not $[Ca^{2+}]_i$ decrease, regardless of the states of TRPC channels. The enriched expression of the NCX isoforms in glioblastoma cells provides a unique target to selectively disrupt intracellular Ca^{2+} homeostasis and induce cytotoxicity in these tumour cells.

Acknowledgements

This work was supported by NIH grants NS0458710, the American Heart Association (AHA) Postdoctoral Fellowship 12POST12080252 (MS) and Grant-in-Aid Award GRNT12060222 (SPY). It was also supported by the NIH grant C06 RR015455 from the Extramural Research Facilities Program of the National Center for Research Resources.

We thank Dr. H. A. Jinnah for facility assistance in calcium imaging experiment.

Conflict of interest

The authors declare that there is no conflict of interest in this study.

References

Abramowitz J, Yildirim E, Birnbaumer L (2007). The TRPC family of ion channels: relation to the TRP superfamily and role in receptor- and store-operated calcium entry. In: Liedtke WB, Heller S (eds). TRP Ion Channel Function in Sensory Transduction and Cellular Signaling Cascades. CRC Press: Boca Raton, FL, pp. 1–26.

Alexander SPH, Benson HE, Faccenda E, Pawson AJ, Sharman JL, Spedding M *et al.* (2013a). The Concise Guide to PHARMACOLOGY 2013/14: Transporters. Br J Pharmacol 170: 1706–1796.

Alexander SPH, Benson HE, Faccenda E, Pawson AJ, Sharman JL, Catterall WA *et al.* (2013b). The Concise Guide to PHARMACOLOGY 2013/14: Ion Channels. Br J Pharmacol 170: 1607–1651.

Amaral MD, Pozzo-Miller L (2007). BDNF induces calcium elevations associated with IBDNF, a non-selective cationic current mediated by TRPC channels. J Neurophysiol 98: 2476–2482.

Annunziato L, Pignataro G, Di Renzo GF (2004). Pharmacology of brain Na^+/Ca^{2+} exchanger: from molecular biology to therapeutic perspectives. Pharmacol Rev 56: 633–654.

Antigny F, Jousset H, Konig S, Frieden M (2011). Thapsigargin activates Ca(2)+ entry both by store-dependent, STIM1/Orai1-mediated, and store-independent, TRPC3/PLC/PKC-mediated pathways in human endothelial cells. Cell Calcium 49: 115–127.

Ashwell JD (2006). The many paths to p38 mitogen-activated protein kinase activation in the immune system. Nat Rev Immunol 6: 532–540.

Berridge MJ, Bootman MD, Lipp P (1998). Calcium – a life and death signal. Nature 395: 645–648.

Berridge MJ, Lipp P, Bootman MD (2000). The versatility and universality of calcium signalling. Nat Rev Mol Cell Biol 1: 11–21.

Blaustein MP, Juhaszova M, Golovina VA, Church PJ, Stanley EF (2002). Na/Ca exchanger and PMCA localization in neurons and astrocytes: functional implications. Ann N Y Acad Sci 976: 356–366.

Bomben VC, Sontheimer HW (2008). Inhibition of transient receptor potential canonical channels impairs cytokinesis in human malignant gliomas. Cell Prolif 41: 98–121.

Brat DJ, Prayson RA, Ryken TC, Olson JJ (2008). Diagnosis of malignant glioma: role of neuropathology. J Neurooncol 89: 287–311.

Cai R, Ding X, Zhou K, Shi Y, Ge R, Ren G *et al.* (2009). Blockade of TRPC6 channels induced G2/M phase arrest and suppressed growth in human gastric cancer cells. Int J Cancer 125: 2281–2287.

Cheng KT, Ong HL, Liu X, Ambudkar IS (2013). Contribution and regulation of TRPC channels in store-operated Ca(2+) entry. Curr Top Membr 71: 149–179.

Chigurupati S, Venkataraman R, Barrera D, Naganathan A, Madan M, Paul L *et al.* (2010). Receptor channel TRPC6 is a key mediator of Notch-driven glioblastoma growth and invasiveness. Cancer Res 70: 418–427.

Clapham DE (2007). Calcium signaling. Cell 131: 1047–1058.

Ding X, He Z, Zhou K, Cheng J, Yao H, Lu D *et al.* (2010). Essential role of TRPC6 channels in G2/M phase transition and development of human glioma. J Natl Cancer Inst 102: 1052–1068.

DiPolo R, Beauge L (2006). Sodium/calcium exchanger: influence of metabolic regulation on ion carrier interactions. Physiol Rev 86: 155–203.

Furnari FB, Fenton T, Bachoo RM, Mukasa A, Stommel JM, Stegh A *et al.* (2007). Malignant astrocytic glioma: genetics, biology, and paths to treatment. Genes Dev 21: 2683–2710.

Gutierrez GJ, Tsuji T, Cross JV, Davis RJ, Templeton DJ, Jiang W *et al.* (2010). JNK-mediated phosphorylation of Cdc25C regulates cell cycle entry and G(2)/M DNA damage checkpoint. J Biol Chem 285: 14217–14228.

Harmar AJ, Hills RA, Rosser EM, Jones M, Buneman OP, Dunbar DR *et al.* (2009). IUPHAR-DB: the IUPHAR database of G protein-coupled receptors and ion channels. Nucleic Acids Res 37 (Database issue): D680–D685.

He LP, Cleemann L, Soldatov NM, Morad M (2003). Molecular determinants of cAMP-mediated regulation of the Na^+-Ca^{2+} exchanger expressed in human cell lines. J Physiol 548 (Pt 3): 677–689.

Hotta A, Kim YC, Nakamura E, Kito Y, Yamamoto Y, Suzuki H (2005). Effects of inhibitors of nonselective cation channels on the acetylcholine-induced depolarization of circular smooth muscle from the guinea-pig stomach antrum. J Smooth Muscle Res 41: 313–327.

Iouzalen L, Lantoine F, Pernollet MG, Millanvoye-Van Brussel E, Devynck MA, David-Dufilho M (1996). SK&F 96365 inhibits intracellular Ca^{2+} pumps and raises cytosolic Ca^{2+} concentration without production of nitric oxide and von Willebrand factor. Cell Calcium 20: 501–508.

Iwamoto T, Kita S (2006). YM-244769, a novel Na^+/Ca^{2+} exchange inhibitor that preferentially inhibits NCX3, efficiently protects against hypoxia/reoxygenation-induced SH-SY5Y neuronal cell damage. Mol Pharmacol 70: 2075–2083.

Jan CR, Ho CM, Wu SN, Tseng CJ (1999). Multiple effects of 1-[beta-[3-(4-methoxyphenyl)propoxy]-4-methoxyphenethyl]-1H-imidazole hydrochloride (SKF 96365) on Ca^{2+} signaling in MDCK cells: depletion of thapsigargin-sensitive Ca^{2+} store followed by capacitative Ca^{2+} entry, activation of a direct Ca^{2+} entry, and inhibition of thapsigargin-induced capacitative Ca^{2+} entry. Naunyn Schmiedebergs Arch Pharmacol 359: 92–101.

Jia Y, Zhou J, Tai Y, Wang Y (2007). TRPC channels promote cerebellar granule neuron survival. Nat Neurosci 10: 559–567.

Kim YT, Park YJ, Jung SY, Seo WS, Suh CK (2005). Effects of Na^+-Ca^{2+} exchanger activity on the alpha-amino-3-hydroxy-5-methyl-4-isoxazolone-propionate-induced Ca^{2+} influx in cerebellar Purkinje neurons. Neuroscience 131: 589–599.

Krex D, Klink B, Hartmann C, von Deimling A, Pietsch T, Simon M *et al.* (2007). Long-term survival with glioblastoma multiforme. Brain 130 (Pt 10): 2596–2606.

Kuhn SA, Mueller U, Hanisch UK, Regenbrecht CR, Schoenwald I, Brodhun M *et al.* (2009). Glioblastoma cells express functional cell membrane receptors activated by daily used medical drugs. J Cancer Res Clin Oncol 135: 1729–1745.

Labelle D, Jumarie C, Moreau R (2007). Capacitative calcium entry and proliferation of human osteoblast-like MG-63 cells. Cell Prolif 40: 866–884.

Lee YS, Sayeed MM, Wurster RD (1994). Inhibition of cell growth and intracellular Ca^{2+} mobilization in human brain tumor cells by Ca^{2+} channel antagonists. Mol Chem Neuropathol 22: 81–95.

Leung YM, Kwan CY, Loh TT (1996). Dual effects of SK&F 96365 in human leukemic HL-60 cells. Inhibition of calcium entry and activation of a novel cation influx pathway. Biochem Pharmacol 51: 605–612.

Li Y, Jia YC, Cui K, Li N, Zheng ZY, Wang YZ *et al.* (2005). Essential role of TRPC channels in the guidance of nerve growth cones by brain-derived neurotrophic factor. Nature 434: 894–898.

Liu H, Hughes JD, Rollins S, Chen B, Perkins E (2011). Calcium entry via ORAI1 regulates glioblastoma cell proliferation and apoptosis. Exp Mol Pathol 91: 753–760.

Lytton J, Westlin M, Hanley MR (1991). Thapsigargin inhibits the sarcoplasmic or endoplasmic reticulum Ca-ATPase family of calcium pumps. J Biol Chem 266: 17067–17071.

Merritt JE, Armstrong WP, Benham CD, Hallam TJ, Jacob R, Jaxa-Chamiec A *et al.* (1990). SK&F 96365, a novel inhibitor of receptor-mediated calcium entry. Biochem J 271: 515–522.

Minelli A, Castaldo P, Gobbi P, Salucci S, Magi S, Amoroso S (2007). Cellular and subcellular localization of Na^+-Ca^{2+} exchanger protein isoforms, NCX1, NCX2, and NCX3 in cerebral cortex and hippocampus of adult rat. Cell Calcium 41: 221–234.

Molinaro P, Cuomo O, Pignataro G, Boscia F, Sirabella R, Pannaccione A *et al.* (2008). Targeted disruption of Na^+/Ca^{2+} exchanger 3 (NCX3) gene leads to a worsening of ischemic brain damage. J Neurosci 28: 1179–1184.

Parsons DW, Jones S, Zhang X, Lin JC, Leary RJ, Angenendt P *et al.* (2008). An integrated genomic analysis of human glioblastoma multiforme. Science 321: 1807–1812.

Rahman M, Inman M, Kiss L, Janssen LJ (2012). Reverse-mode NCX current in mouse airway smooth muscle: Na(+) and voltage dependence, contributions to Ca(2+) influx and contraction, and altered expression in a model of allergen-induced hyperresponsiveness. Acta Physiol (Oxf) 205: 279–291.

Rao JS (2003). Molecular mechanisms of glioma invasiveness: the role of proteases. Nat Rev Cancer 3: 489–501.

Roderick HL, Cook SJ (2008). Ca^{2+} signalling checkpoints in cancer: remodelling Ca^{2+} for cancer cell proliferation and survival. Nat Rev Cancer 8: 361–375.

Rosen LB, Ginty DD, Weber MJ, Greenberg ME (1994). Membrane depolarization and calcium influx stimulate MEK and MAP kinase via activation of Ras. Neuron 12: 1207–1221.

Schwarz G, Droogmans G, Nilius B (1994). Multiple effects of SK&F 96365 on ionic currents and intracellular calcium in human endothelial cells. Cell Calcium 15: 45–54.

See V, Rajala NK, Spiller DG, White MR (2004). Calcium-dependent regulation of the cell cycle via a novel MAPK – NF-kappaB pathway in Swiss 3T3 cells. J Cell Biol 166: 661–672.

Smyth JT, Dehaven WI, Jones BF, Mercer JC, Trebak M, Vazquez G *et al.* (2006). Emerging perspectives in store-operated Ca^{2+} entry: roles of Orai, Stim and TRP. Biochim Biophys Acta 1763: 1147–1160.

Sokolow S, Luu SH, Headley AJ, Hanson AY, Kim T, Miller CA *et al.* (2011). High levels of synaptosomal Na(+)-Ca(2+) exchangers (NCX1, NCX2, NCX3) co-localized with amyloid-beta in human cerebral cortex affected by Alzheimer's disease. Cell Calcium 49: 208–216.

Stupp R, Mason WP, van den Bent MJ, Weller M, Fisher B, Taphoorn MJ *et al.* (2005). Radiotherapy plus concomitant and adjuvant temozolomide for glioblastoma. N Engl J Med 352: 987–996.

Thurneysen T, Nicoll DA, Philipson KD, Porzig H (2002). Sodium/calcium exchanger subtypes NCX1, NCX2 and NCX3 show cell-specific expression in rat hippocampus cultures. Brain Res Mol Brain Res 107: 145–156.

Van Meir E, Sawamura Y, Diserens AC, Hamou MF, de Tribolet N (1990). Human glioblastoma cells release interleukin 6 in vivo and in vitro. Cancer Res 50: 6683–6688.

Van Meir E, Ceska M, Effenberger F, Walz A, Grouzmann E, Desbaillets I *et al.* (1992). Interleukin-8 is produced in neoplastic and infectious diseases of the human central nervous system. Cancer Res 52: 4297–4305.

Van Meir EG, Hadjipanayis CG, Norden AD, Shu HK, Wen PY, Olson JJ (2010). Exciting new advances in neuro-oncology: the avenue to a cure for malignant glioma. CA Cancer J Clin 60: 166–193.

Varnai P, Hunyady L, Balla T (2009). STIM and Orai: the long-awaited constituents of store-operated calcium entry. Trends Pharmacol Sci 30: 118–128.

Verkhratsky A, Orkand RK, Kettenmann H (1998). Glial calcium: homeostasis and signaling function. Physiol Rev 78: 99–141.

Verkhratsky A, Rodriguez JJ, Parpura V (2012). Calcium signalling in astroglia. Mol Cell Endocrinol 353: 45–56.

Wang GX, Poo MM (2005). Requirement of TRPC channels in netrin-1-induced chemotropic turning of nerve growth cones. Nature 434: 898–904.

Yang S, Zhang JJ, Huang XY (2009). Orai1 and STIM1 are critical for breast tumor cell migration and metastasis. Cancer Cell 15: 124–134.

Yu SP, Choi DW (1997). Na(+)-Ca^{2+} exchange currents in cortical neurons: concomitant forward and reverse operation and effect of glutamate. Eur J Neurosci 9: 1273–1281.

Zhou X, Wei J, Song M, Francis K, Yu SP (2011). Novel role of KCNQ2/3 channels in regulating neuronal cell viability. Cell Death Differ 18: 493–505.